Electronic Supplementary Material (ESI) for Nanoscale.
This journal is © The Royal Society of Chemistry 2023

Light-gated specific oxidase-like activity of self-assembled Pt(II) nanozyme for environmental remediation

Rohit Kapila,[1] Bhaskar Sen,[1] Alisha Kamra,[1] Shana Chandran,[1] and Subinoy Rana[1]*

[1]Materials Research Centre, Indian Institute of Science, C. V. Raman Road, Bangalore 560012, Karnataka, India

***Corresponding author**

Dr. Subinoy Rana

E-mail: subinoy@iisc.ac.in

Phone: 080-22932914

Instrumentation

^{1}H and ^{13}C NMR spectra were recorded on Bruker Ultrashield AV400 (400 MHz) and Bruker AV500 (500 MHz) high-resolution multinuclear FT-NMR spectrometers and chemical shifts were expressed in ppm using a residual protic solvent as the internal standard. All the NMR data were processed in MestreNova Lite software. The ESI-HRMS of ligands were recorded on a Xevo G2-XS Q-TOF instrument. Whereas, the mass of metal complexes was recorded on an Agilent 6540 UHD Accurate-Mass Q-TOF spectrometer. The UV-Vis absorption spectra, photoluminescence (PL) spectra, and kinetic analyses were acquired at room temperature using a Molecular Devices SpectraMax® M5e microplate reader. The absolute luminescence quantum yield was acquired by Quanta-ϕ Horiba Instrument linked with a Fluorolog spectrophotometer. The luminescence lifetimes were collected on a time-correlated single photon counting (TCSPC) lifetime fluorometer from DeltaPro^{Tm} (HORIBA Scientific). DLS measurement was performed on a Malvern Zetasizer Nano instrument. Field emission scanning electron microscope (FESEM) images were acquired using the Ultra55 FE-SEM Karl Zeiss EDS instrument with 5.0 kV emission voltage.

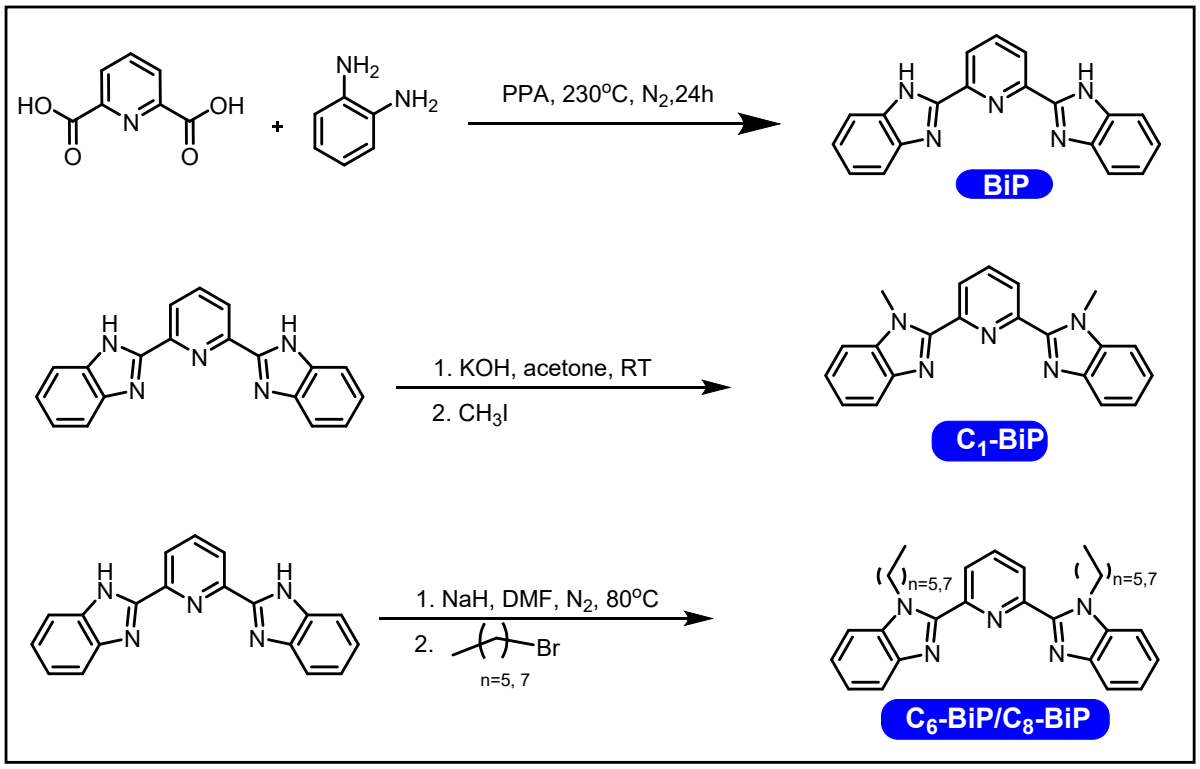

Scheme S1. Synthetic scheme of **BiP**, **C_6-BiP**, and **C8-BiP** ligands.

BiP: ^{1}H NMR (400 MHz, DMSO-d_6)**:** δ (ppm) = 13.00 (bs, 2H), 8.35 (d, J = 8.3 Hz, 2H), 8.15 (t, J = 8.5 Hz, 1H), 7.76 (t, J = 4.4 Hz, 4H), 7.33-7.30 (m, 4H). **^{13}C NMR** (100 MHz, DMSO-d_6)**:** δ (ppm) = 150.9, 148.2, 139.6, 123.6, 121.8. **HRMS (ESI)** $[C_{19}H_{13}N_5 + H]^+$: calcd m/z 312.1244, found m/z 312.1245**.**

C6-BiP: ^{1}H NMR (400 MHz,f DMSO-d_6): δ(ppm) = 8.31 (d, J = 7.9 Hz, 2H), 8.02 (t, J = 7.9 Hz, 1H), 7.88-7.84 (m, 2H), 7.45-7.43 (m, 2H), 7.35-7.29 (m, 4H), 4.68 (t, J = 7.5 Hz, 4H), 1.75-1.68 (m, 4H), 1.08-1.00 (m, 12H), 0.61 (t, J = 6.5 Hz, 3H) . **^{13}C NMR** (100 MHz, DMSO-d_6): δ(ppm) = 150.2, 150.0, 142.8, 138.1, 136.3, 125.5, 123.5, 122.7, 120.3, 110.3, 44.9, 31.1 ,30.0, 26.3, 22.3, 13.7. **HRMS (ESI**) $[C_{21}H_{17}N_5 + H]^+$: calcd m/z 480.3122, found m/z 480.3127.

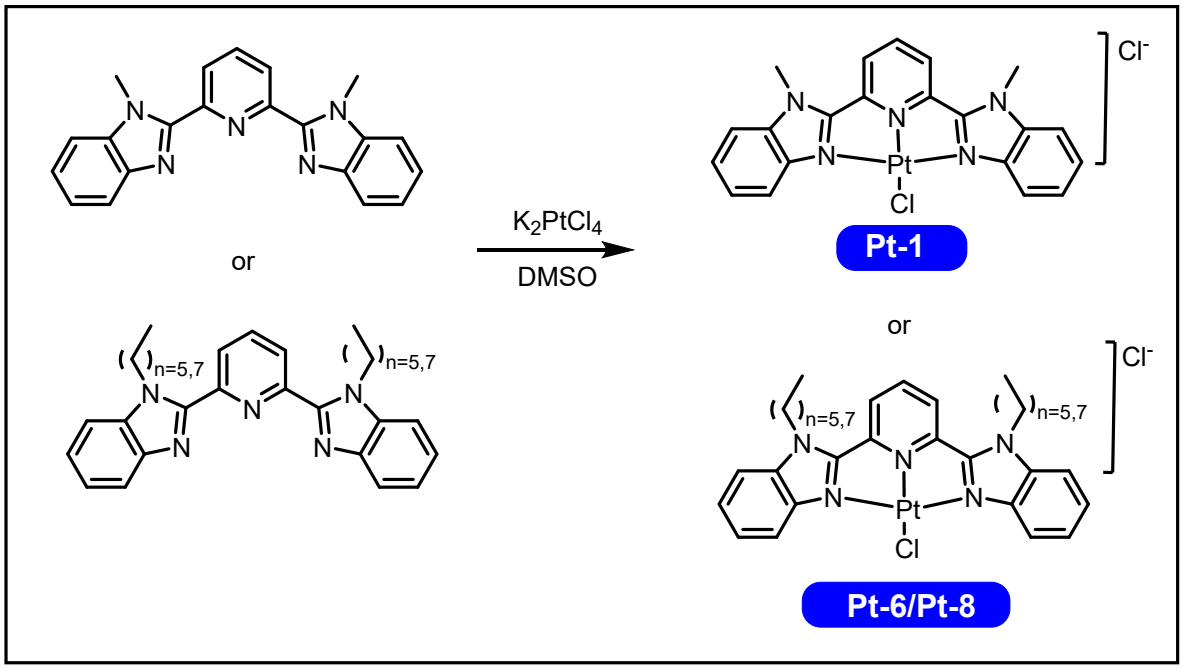

Scheme S2. Synthetic scheme of **Pt-1, Pt-6** and **Pt-8**.

Pt-6- ^{1}H NMR (400 MHz, DMSO-d6) δ 8.45 (t, *J* = 8.1 Hz, 1H), 8.18 (d, *J* = 8.3 Hz, 2H), 7.60 (d, *J* = 8.5 Hz, 2H), 7.46 (d, *J* = 8.2 Hz, 2H), 7.34 (t, *J* = 7.7 Hz, 2H), 7.07 (t, *J* = 7.5 Hz, 2H), 4.31 (t, *J* = 6.5 Hz, 4H), 1.74-1.67 (m, 4H), 1.41-1.26 (m, 12H), 0.90 (t, *J* = 6.9 Hz, 6H). **^{13}C NMR (100 MHz, DMSO-d6)** δ 151.8, 146.9, 138.0, 133.5, 126.4, 126.0, 123.9, 115.36, 112.5, 40.4, 30.8, 29.6, 25.3, 21.9, 13.8. Calculated mass with isotopic distribution as shown in inset Fig. S9.

Pt-1- ^{1}H NMR (400 MHz, DMSO-d_6): δ 8.49 (t, *J* = 8.1 Hz, 1H), 8.31 (d, *J* = 8.1 Hz, 2H), 7.44 (d, *J* = 8.0 Hz, 2H), 7.28 (t, *J* = 7.4 Hz, 2H), 7.16 (t, *J* = 7.6 Hz, 2H), 6.94 (d, *J* = 8.1 Hz, 2H), 3.81 (s, 6H). **^{13}C NMR** (**100 MHz, DMSO-*d_6***): δ(ppm) = 53.1, 147.6, 142.9, 138.2, 133.9, 126.8, 126.0, 125.2, 115.5, 112.6, 32.7. **HRMS (ESI)** $[C_{21}H_{17}ClN_5Pt]^+$: calcd *m/z* 569.0815, found *m/z* 569.0809

Pt-8- ^{1}H NMR (400 MHz, $CDCl_3$): δ 8.95 (bs,1H), 8.42 (bs, 2H), 7.64 (d, *J* = 8.0 Hz, 2H), 7.26m (t, *J* = 7.1 Hz, 2H), 7.12 (t, *J* = 7.1 Hz, 2H), 6.89 (d, *J* = 8.1 Hz, 2H), 4.5 (bs, 4H) ,1.84 (bs, 6H), 1.44-1.26 (m,18H), 0.87 (s, *J* = 7.1 Hz, 6H). **^{13}C NMR (100 MHz, $CDCl_3$)** δ 152.2, 147.3, 139.0, 133.9, 126.8, 125.9, 124.8, 117.1, 111.1, 44.5, 31.8, 30.4, 29.33, 29.1, 22.6,14.1 Calculated mass with isotopic distribution as shown in inset Fig. S9.

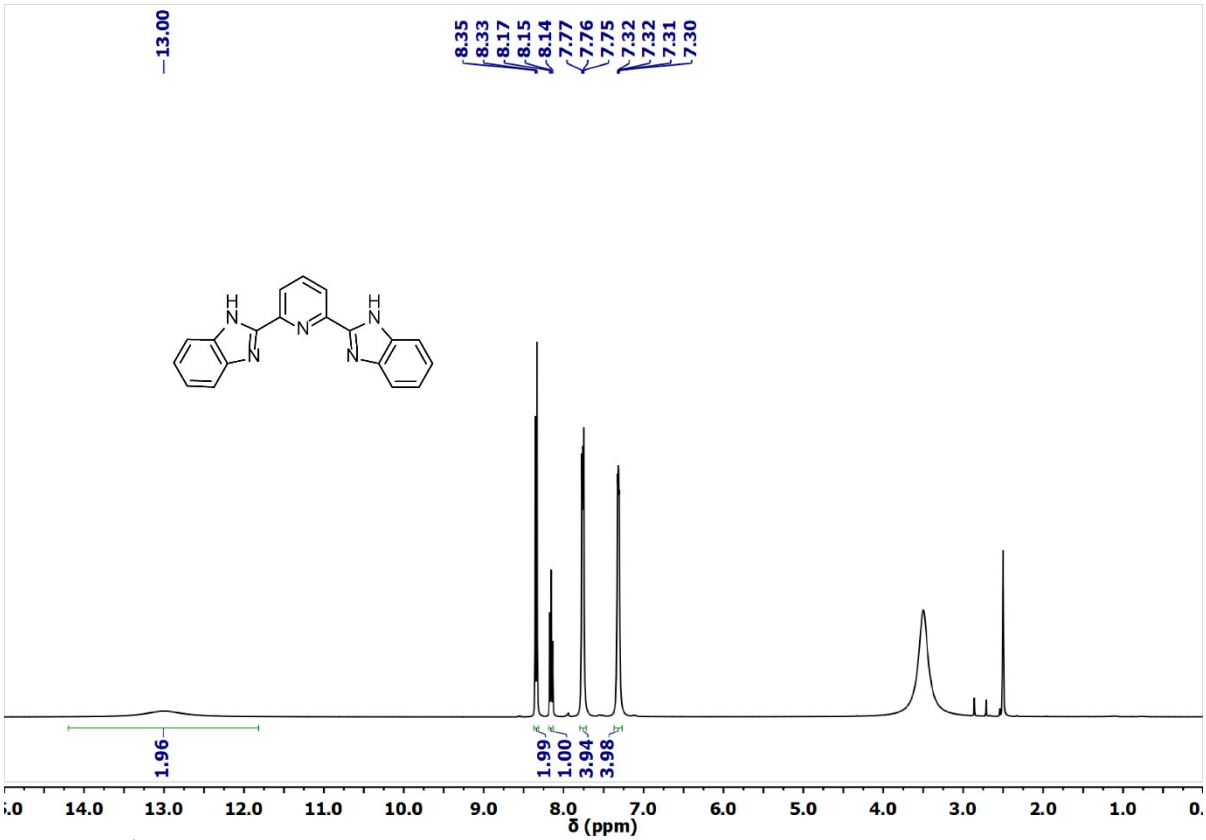

Fig. S1. ^{1}H NMR spectrum of **BiP** in DMSO-d_6.

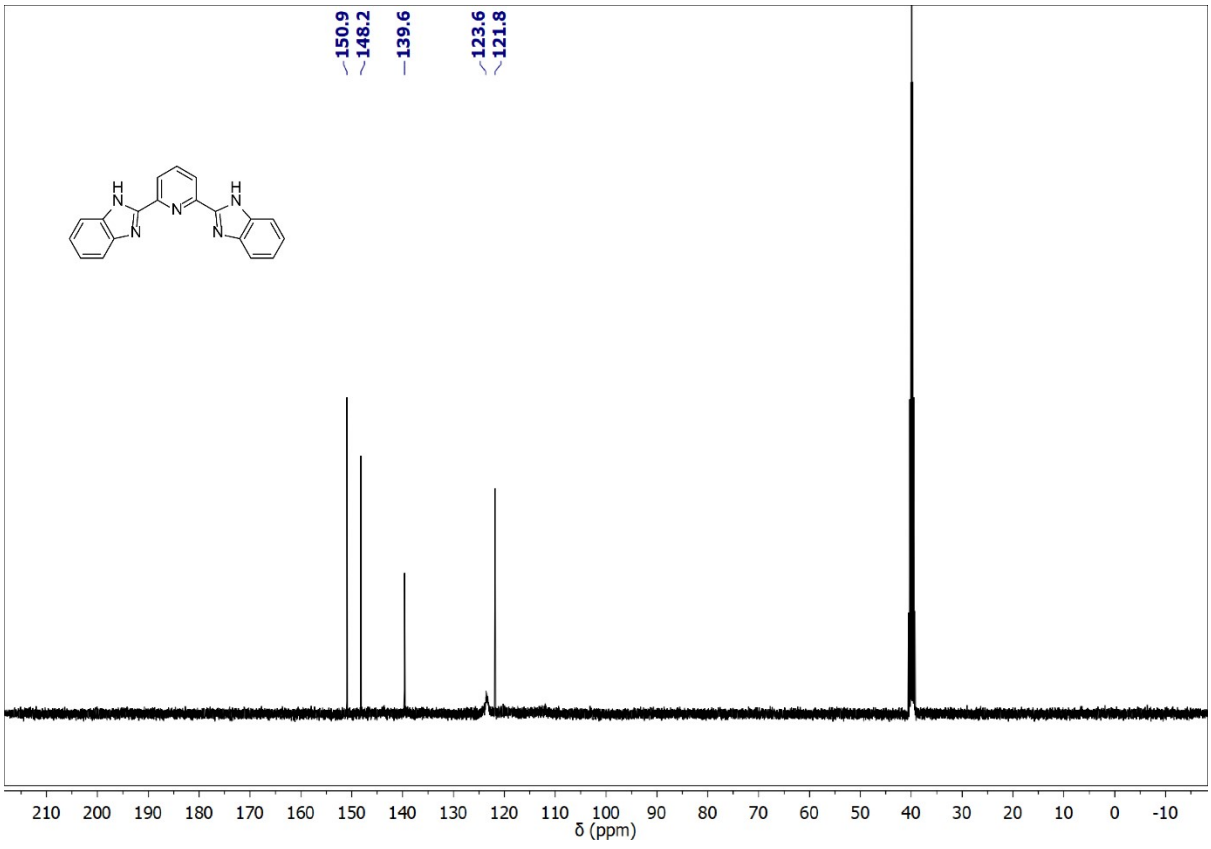

Fig. S2. ^{13}C NMR spectrum of **BiP** in DMSO-d_6.

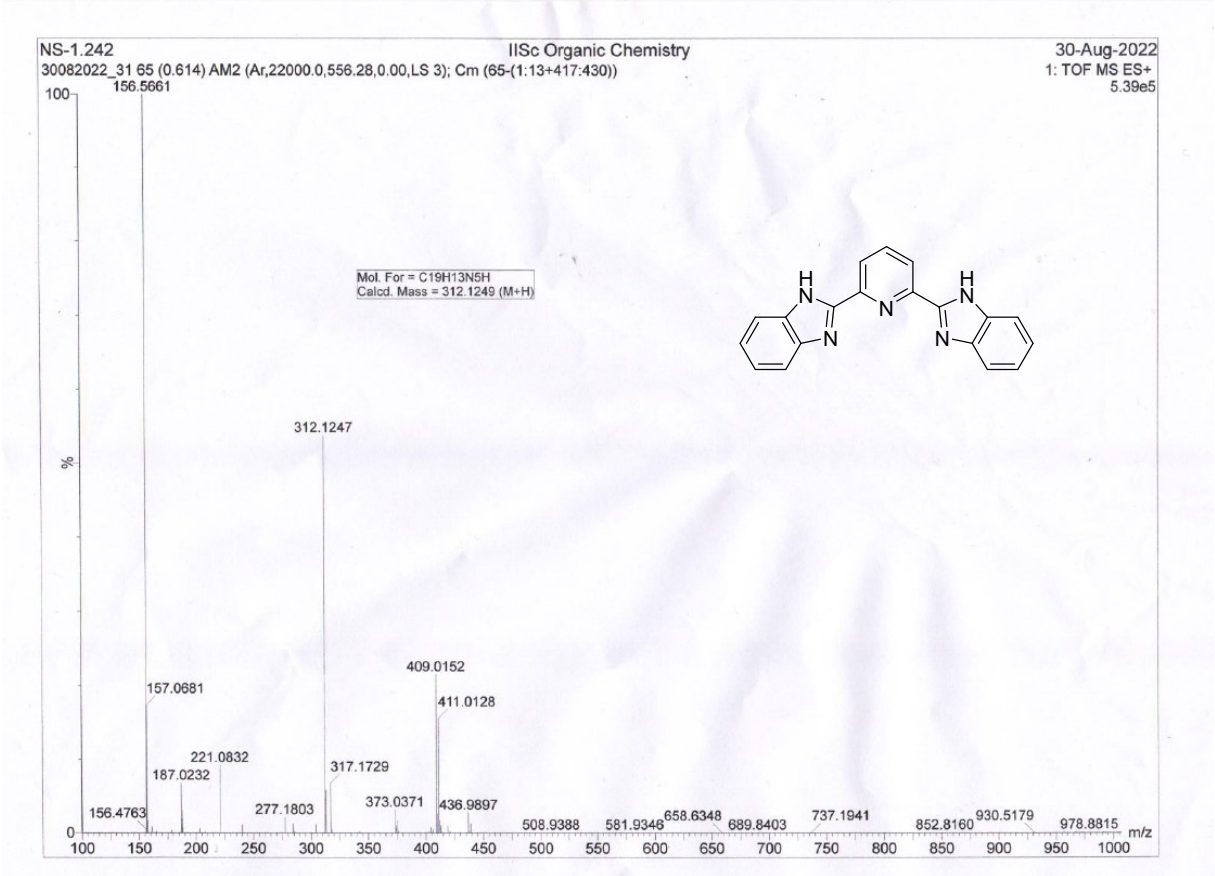

Fig. S3. ESI-HRMS of **C6-BiP**

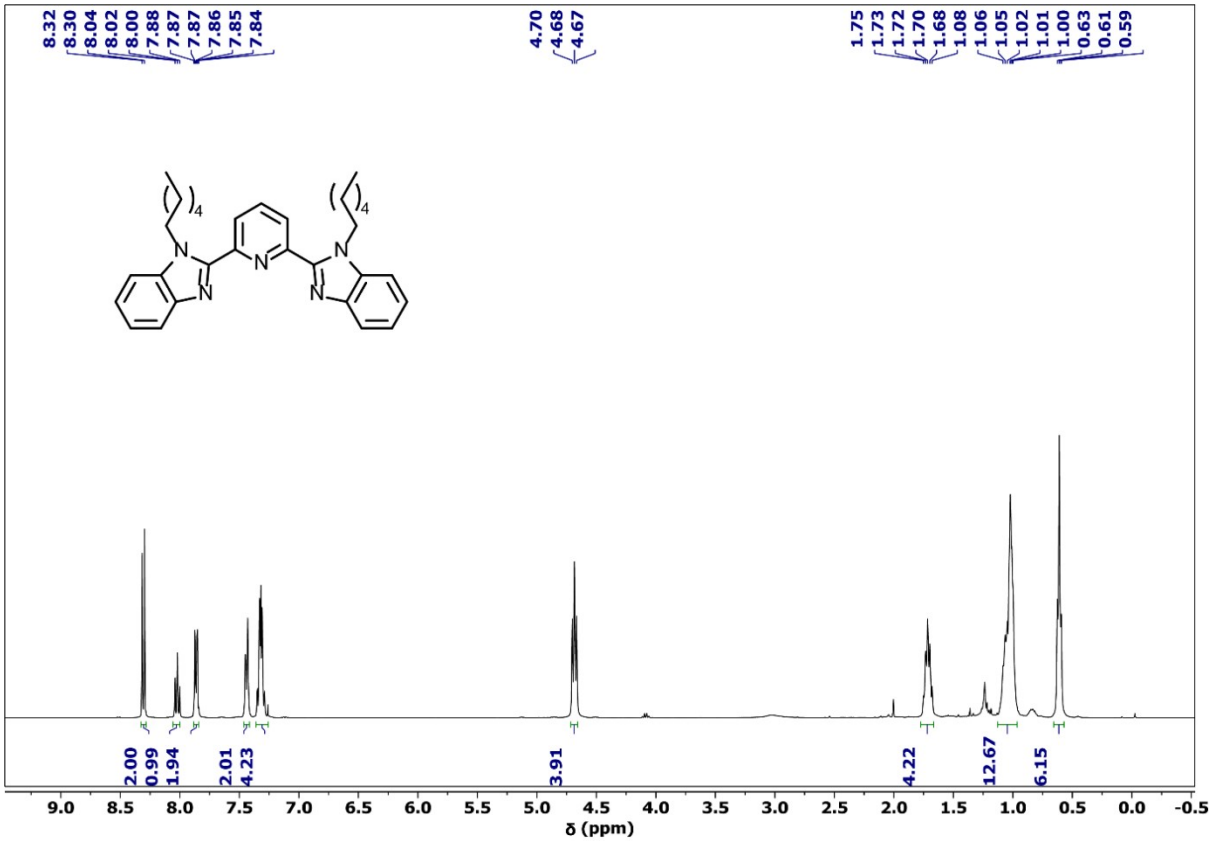

Fig. S4. ^{1}H NMR spectrum of **C6-BiP** in $CDCl_3$.

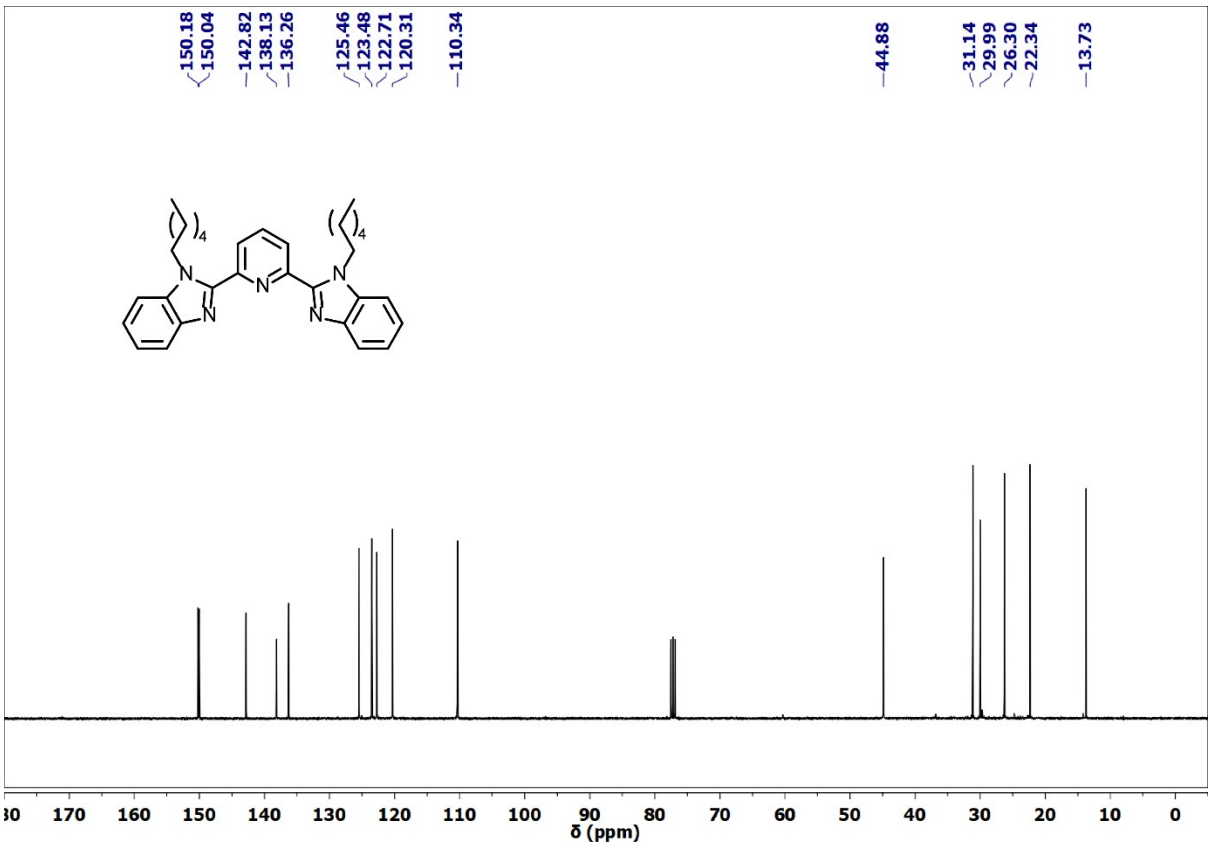

Fig. S5. ^{13}C NMR spectrum of **C6-BiP** in $CDCl_3$.

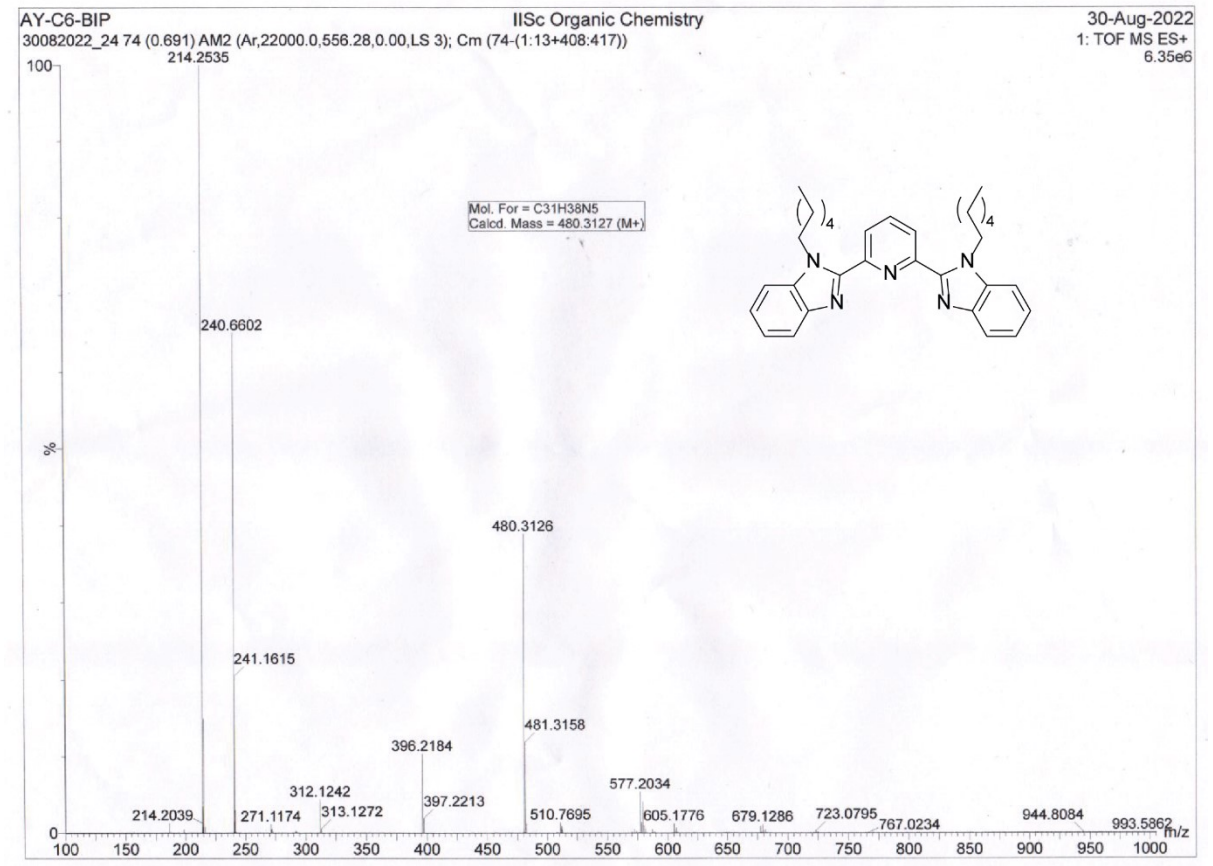

Fig. S6. ESI-HRMS of **C6-BiP.**

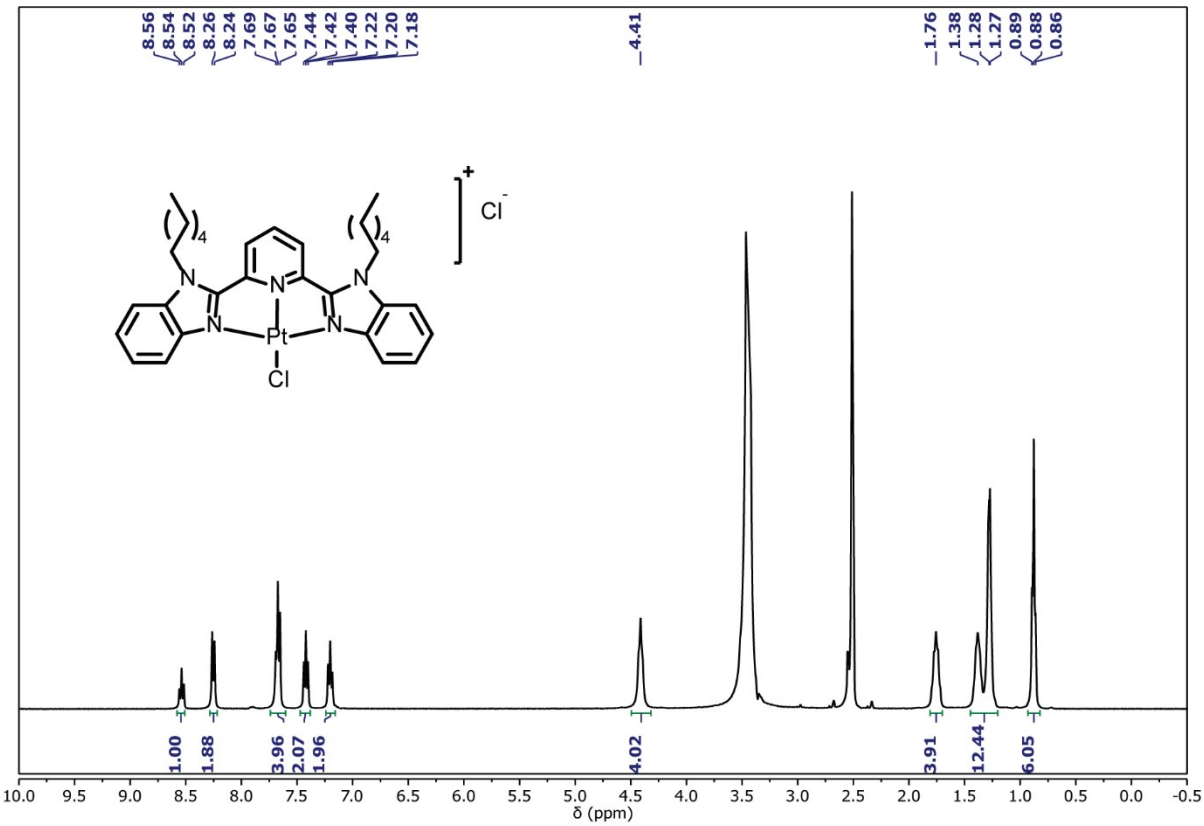

Fig. S7. ^{1}H NMR spectrum of **Pt-6** in DMSO-d_6.

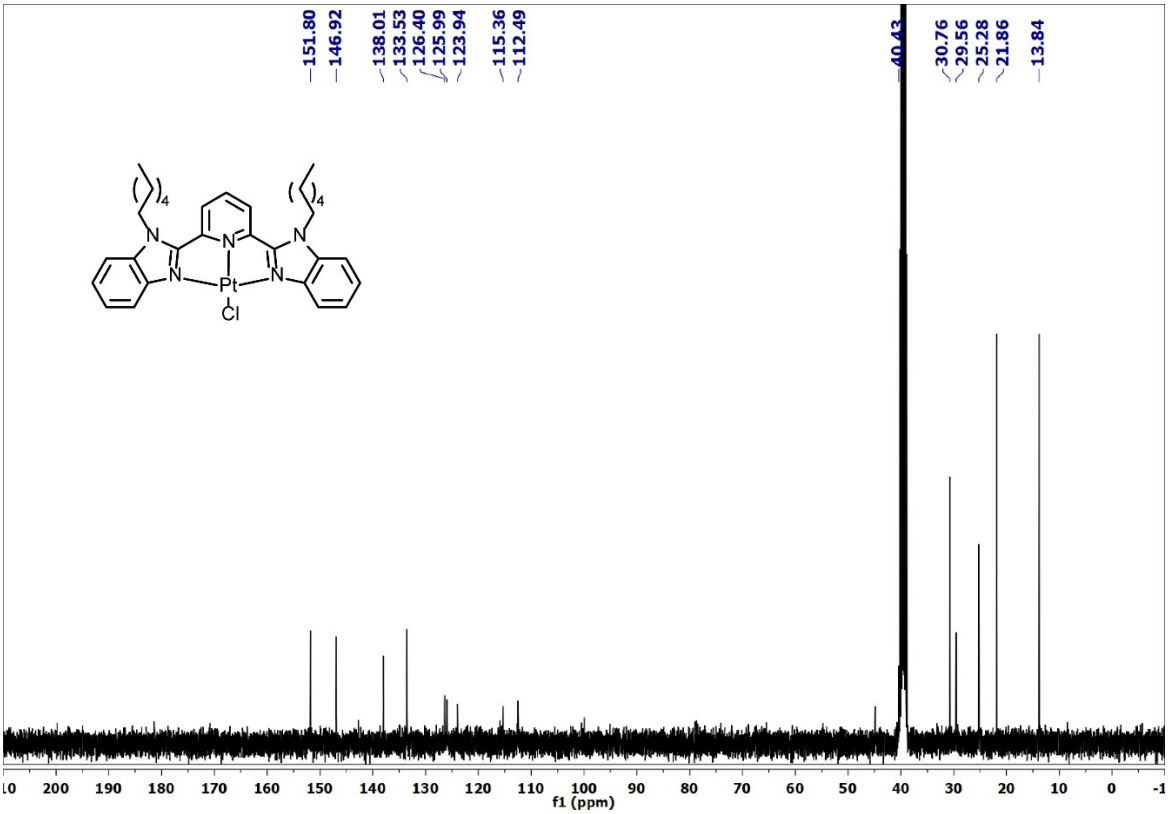

Fig. S8. ^{13}C NMR spectrum of **Pt-6** in DMSO-d_6.

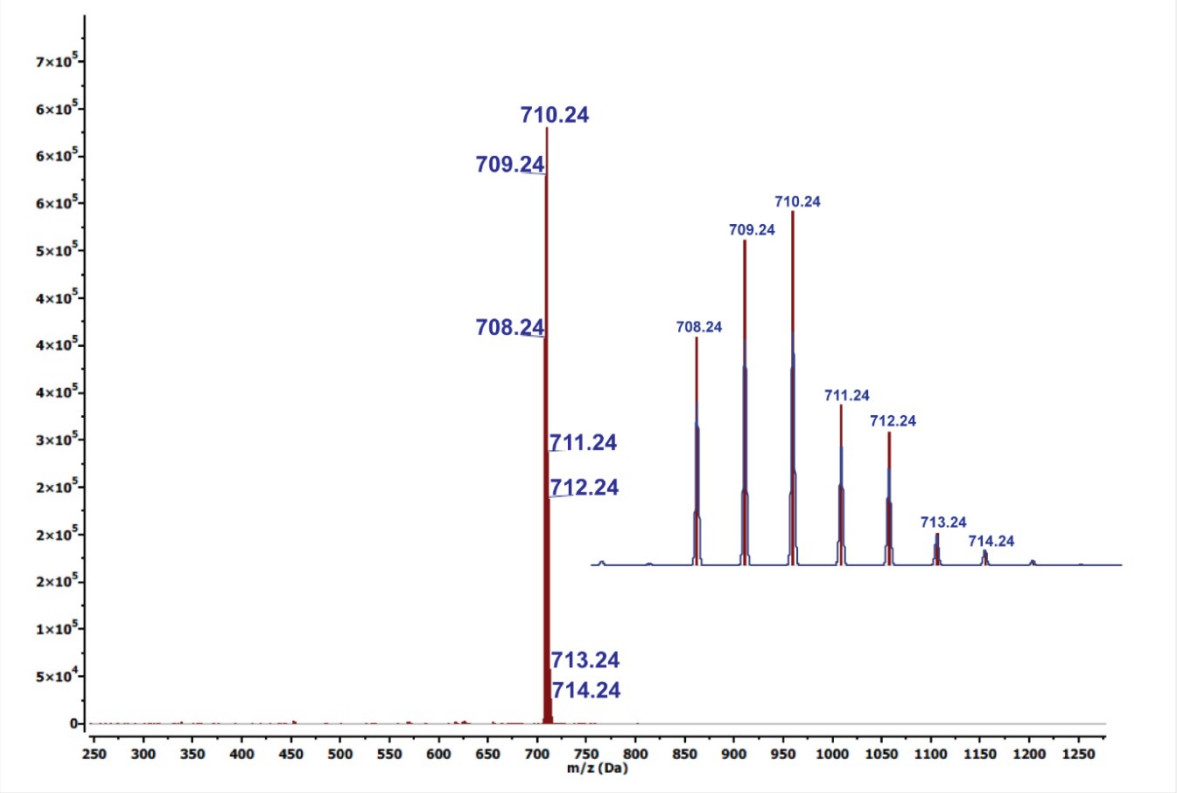

Fig. S9. ESI-MS of **Pt-6**. Inset: isotopic mass distribution pattern of **Pt-6**. Colour code: maroon corresponds to experimentally obtained and blue corresponds to theoretically simulated.

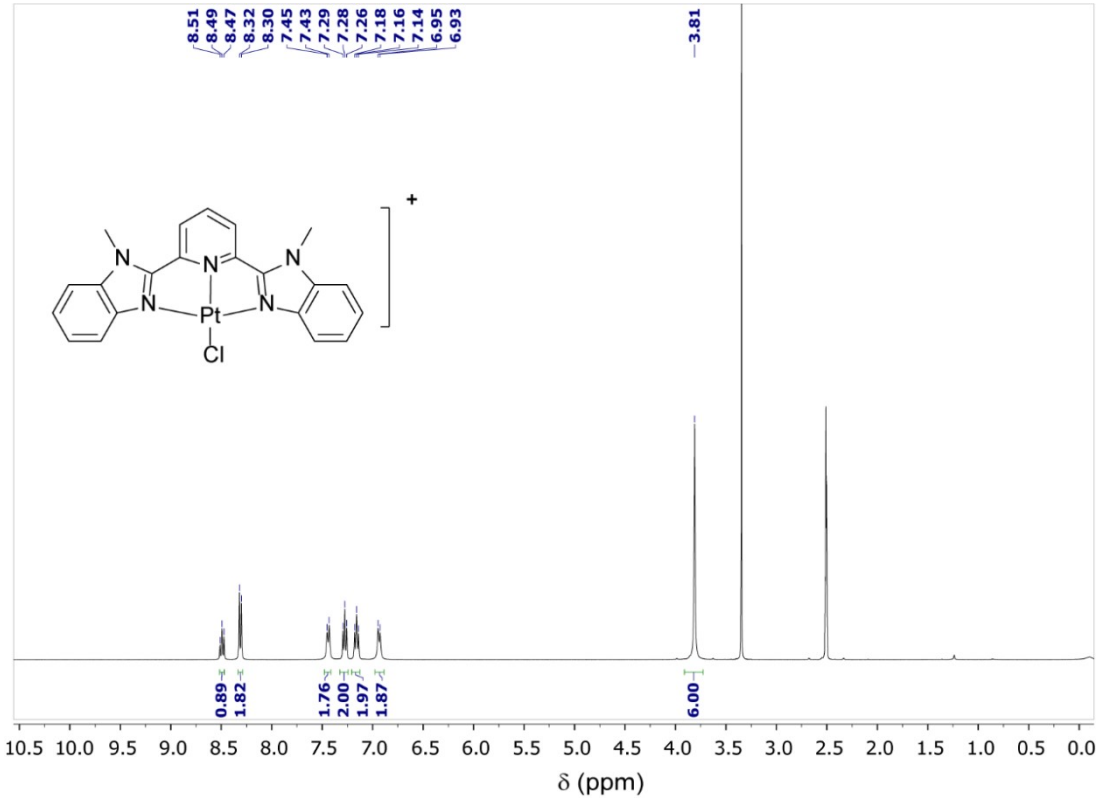

Fig. S10a. ^{1}H NMR spectrum of **Pt-1** in DMSO-d_6.

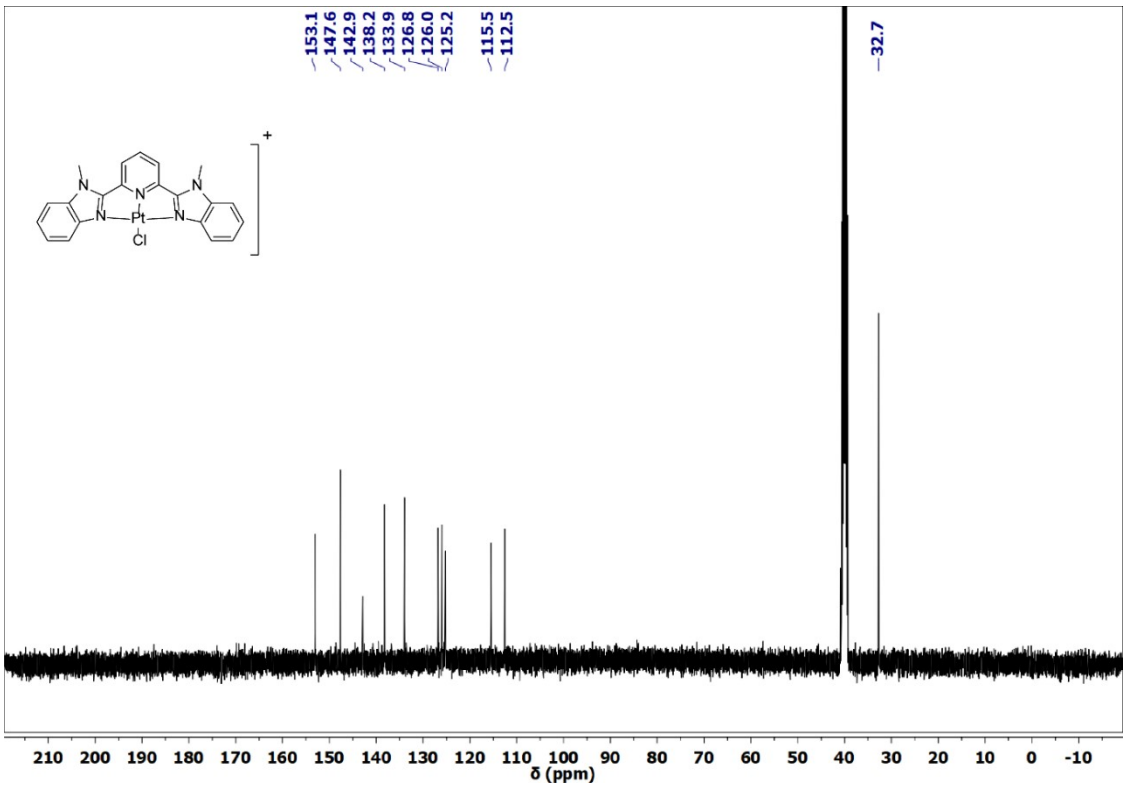

Fig. S10b. ^{13}C NMR spectrum of **Pt-1** in DMSO-d_6.

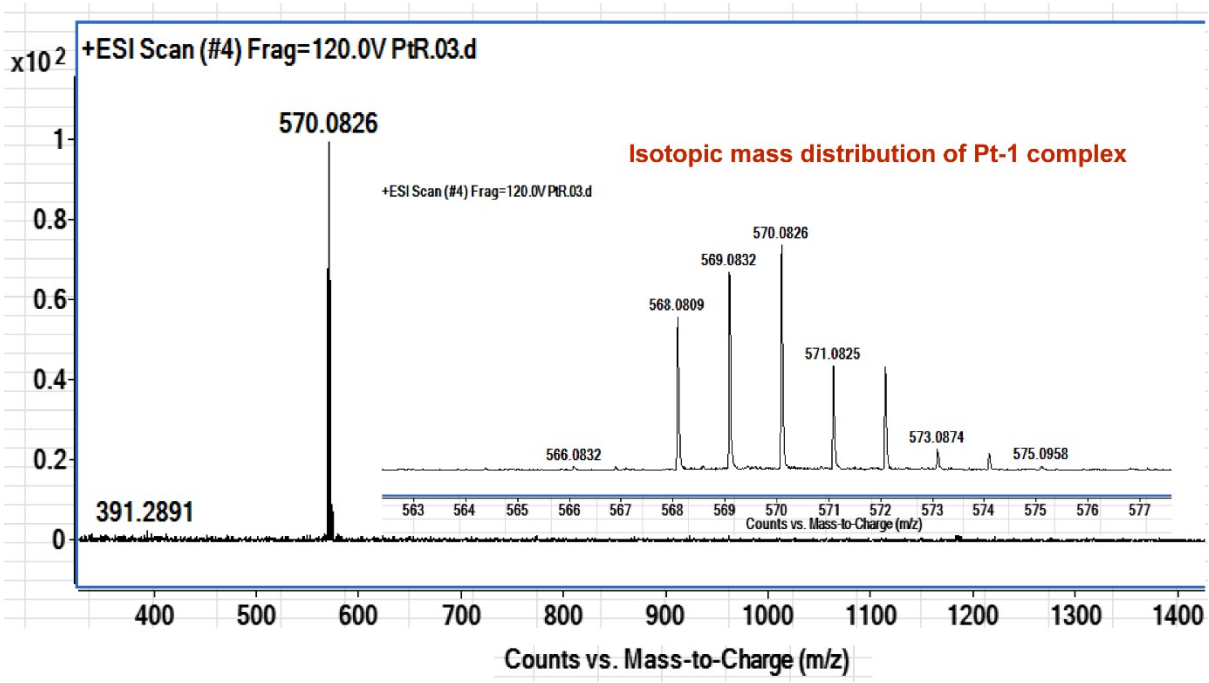

Fig.S10c. ESI-MS of **Pt-1**. Inset: isotopic mass distribution pattern of **Pt-1**

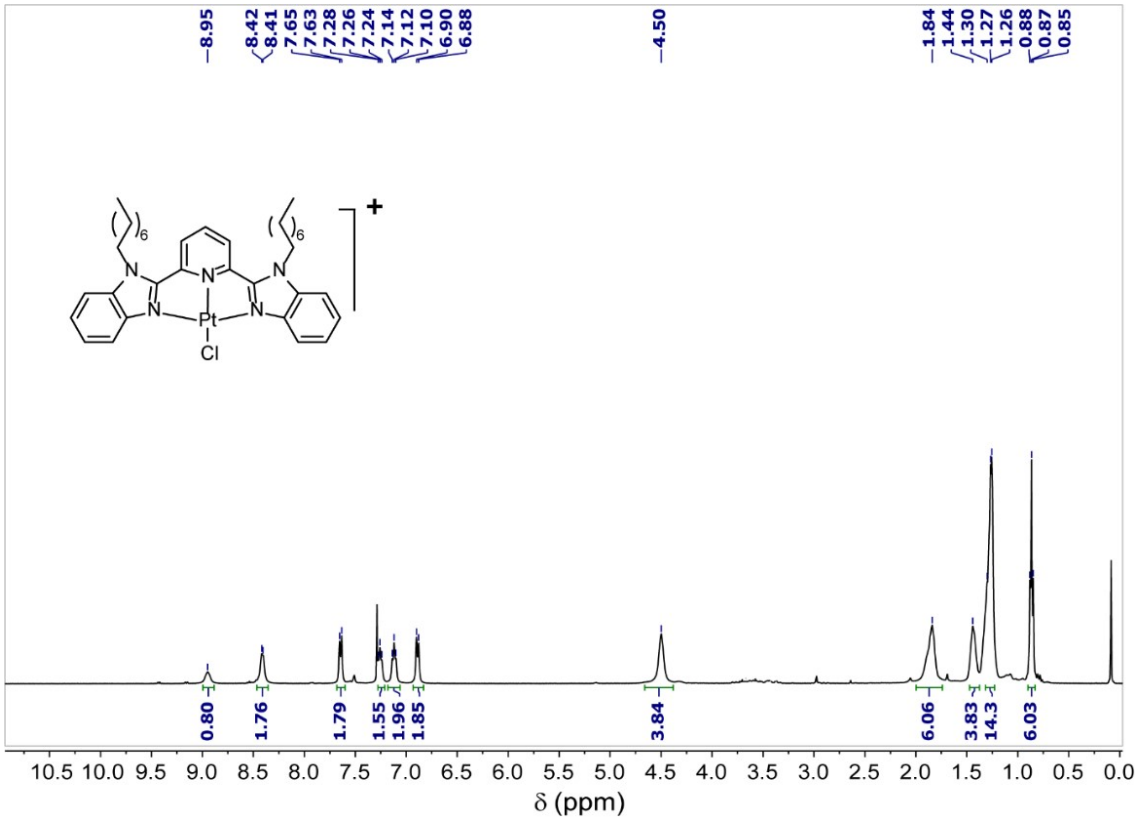

Fig. S11a. ^{1}H NMR spectrum of **Pt-8** in $CDCl_3$.

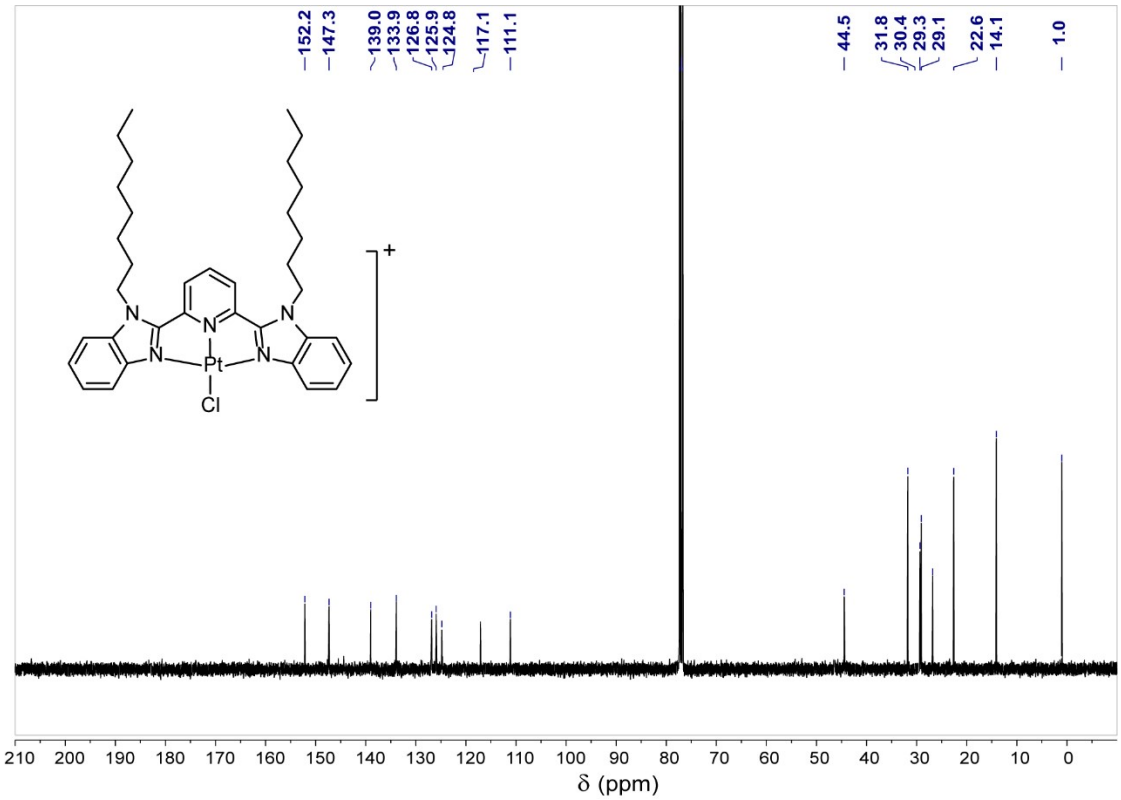

Fig. S11b. ^{13}C NMR spectrum of **Pt-8** in $CDCl_3$.

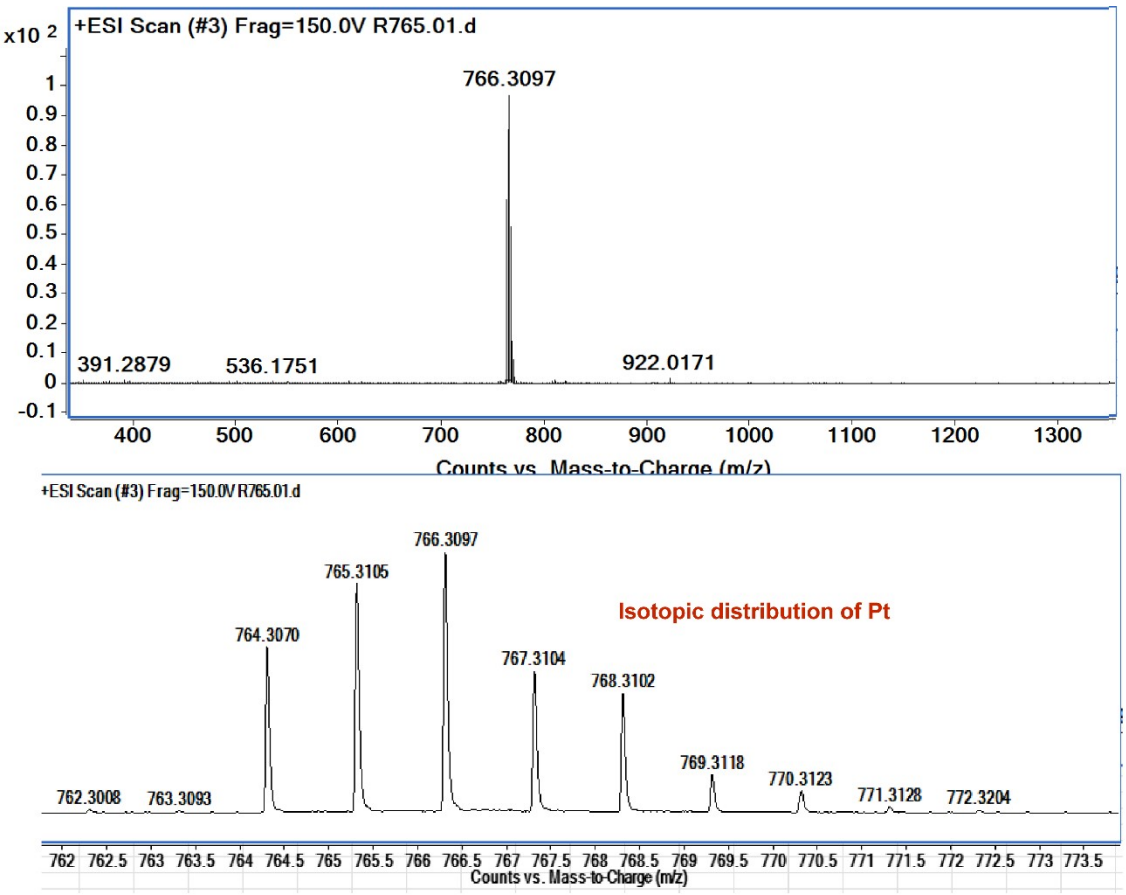

Fig. S11c. ESI-MS of **Pt-8**. down: isotopic mass distribution pattern of **Pt-8.**

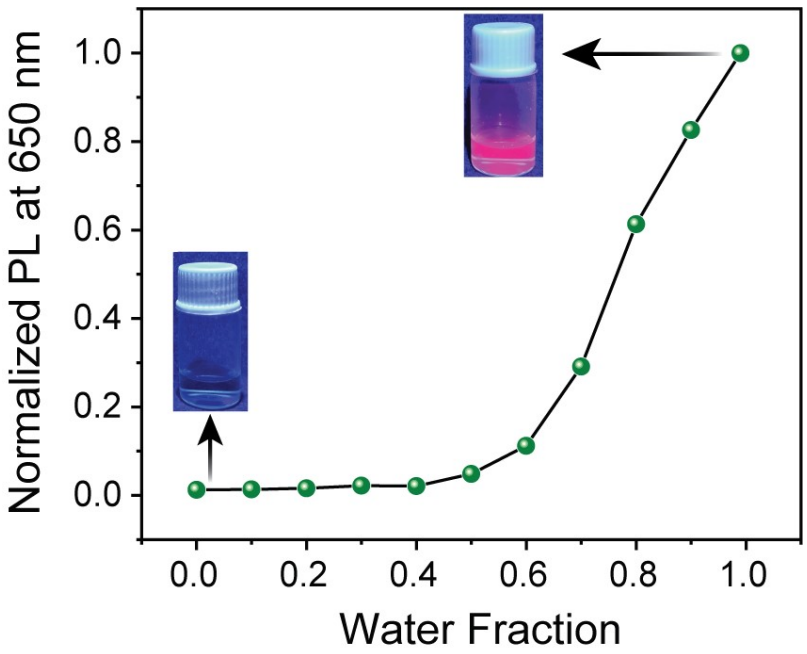

Fig. S12. Normalized PL intensity of **Pt-6** at 650 nm with the increase in water fraction (0-0.99; v/v).

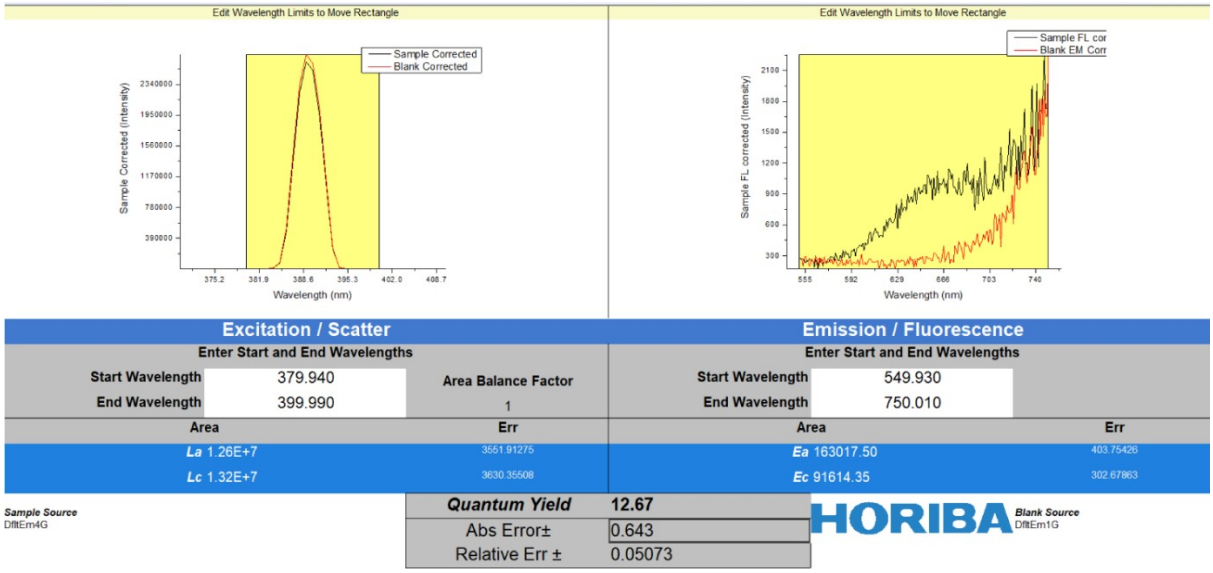

Fig. S13. Absolute luminescence quantum yield of **NanoPtA**

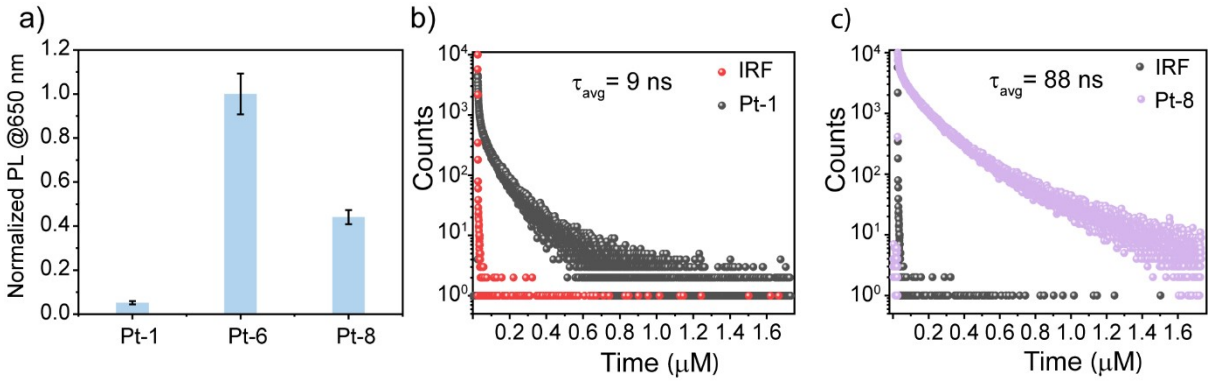

Fig. S14. (a) Bar plot of normalized PL intensity of **Pt-1**, **Pt-6**, and **Pt-8** (10 μM) complexes at 650 nm in 99% water-methanol mixture. Luminescence lifetime of (b) **Pt-1** and (c) **Pt-8** in 99% water-methanol solution, whereas IRF is the instrument response function.

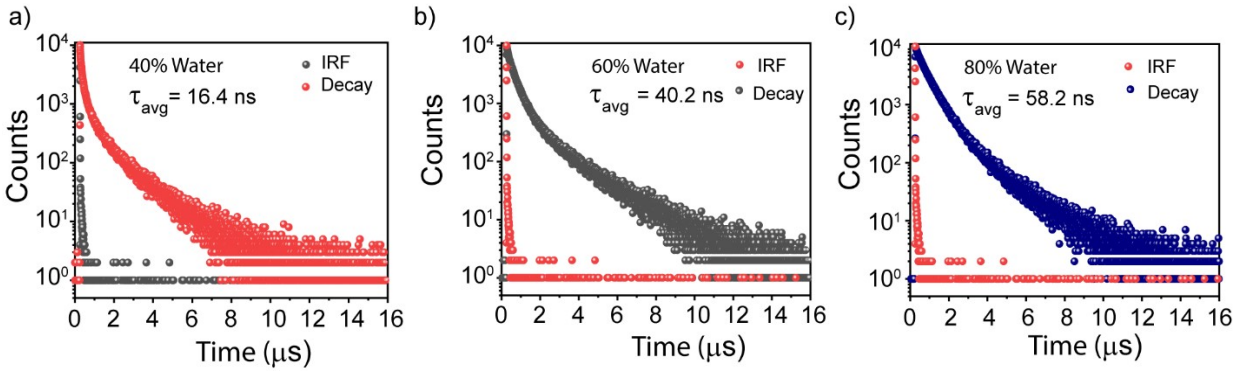

Fig. S15. Photoluminescence lifetime of **Pt-6** at (a) 40%, (b) 60%, and (c) 80% water fractions, whereas IRF is the instrument response function.

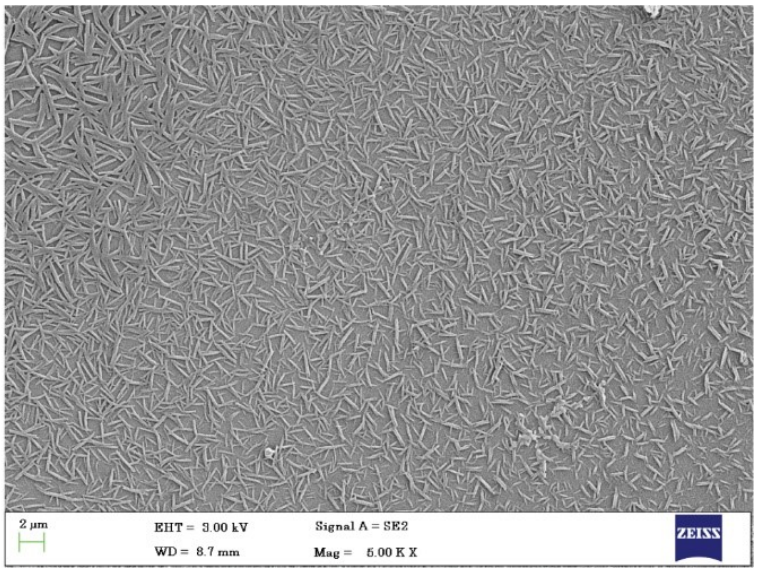

Fig. S16. FESEM images of **NanoPtA** assembly formed in 99% water-methanol mixture.

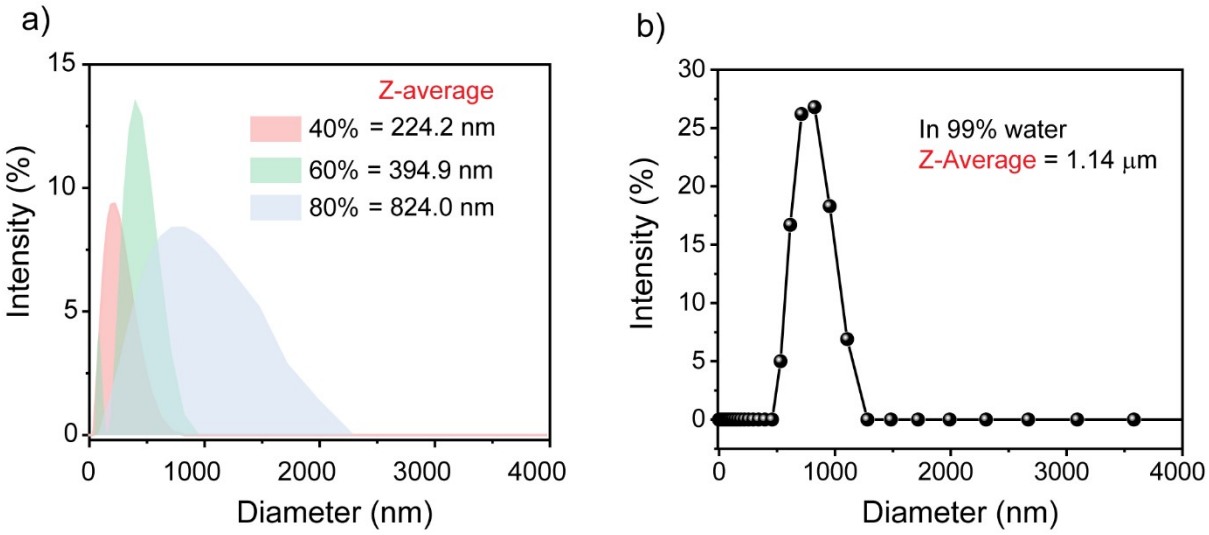

Fig. S17. (a) Particle size distribution of **NanoPtA** in different water fractions at 40%, 60%, and 80 % water-methanol mixture and (b) at 99% water-methanol mixture.

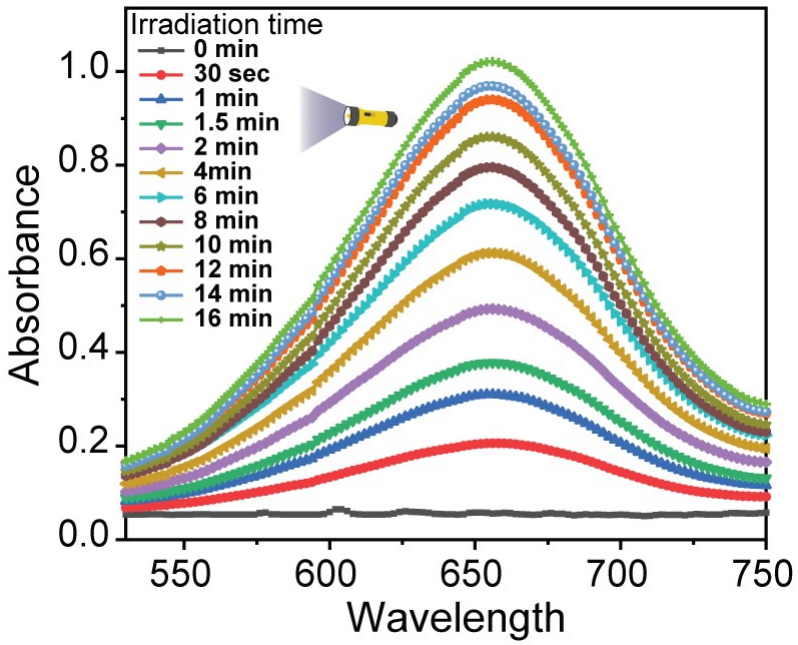

Fig. S18. UV absorption spectra of TMB (0.5 mM) in the presence of **NanoPtA** (10 μM) with the variation of visible light (at 470 nm) exposure time (0-16 min.) in acetate buffer (100 mM, pH 4.0).

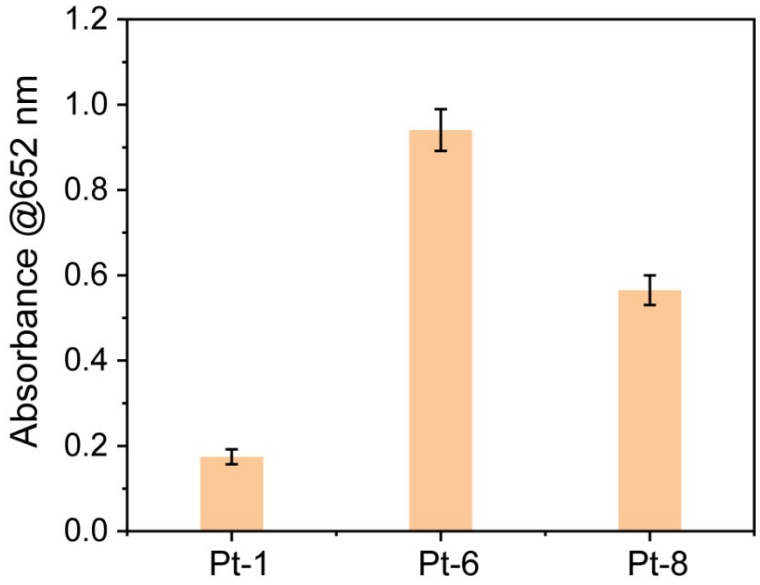

Fig. S19. Absorbance (at 652 nm) of TMB (0.5 mM) oxidized product upon visible light (470 nm) irradiation for 10 min in the presence of **Pt-1**, **Pt-6**, and **Pt-8** in acetate buffer (100 mM, pH 4.0).

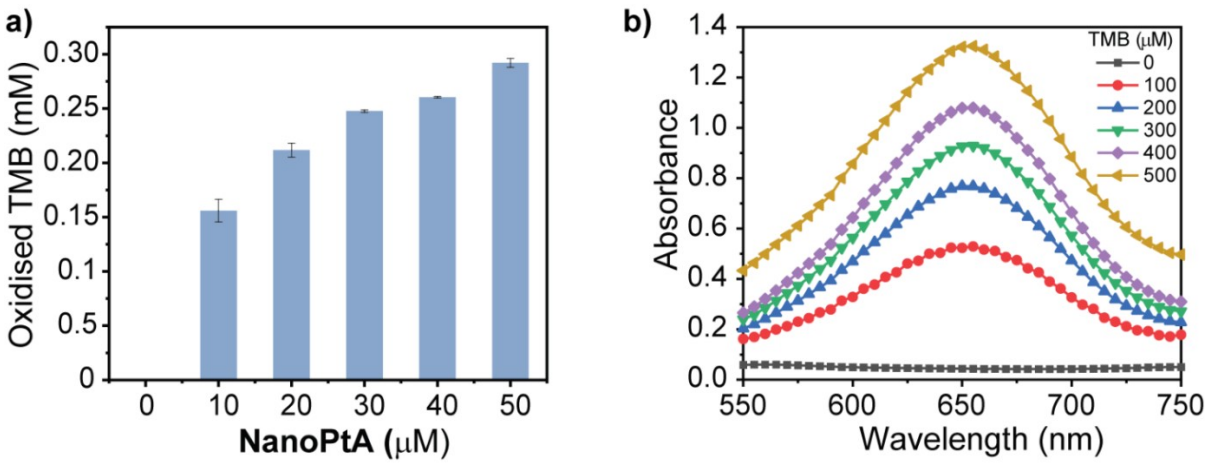

Fig. S20. (a) Extent of TMB oxidation with different concentrations **NanoPtA** (0-50 μM). (b) Absorbance plot of oxidized TMB with increasing concentration of **NanoPtA** (0-500 μM). Condition: medium: acetate buffer (100 mM, pH 4.0) and irradiation of sunlight for 10 min.

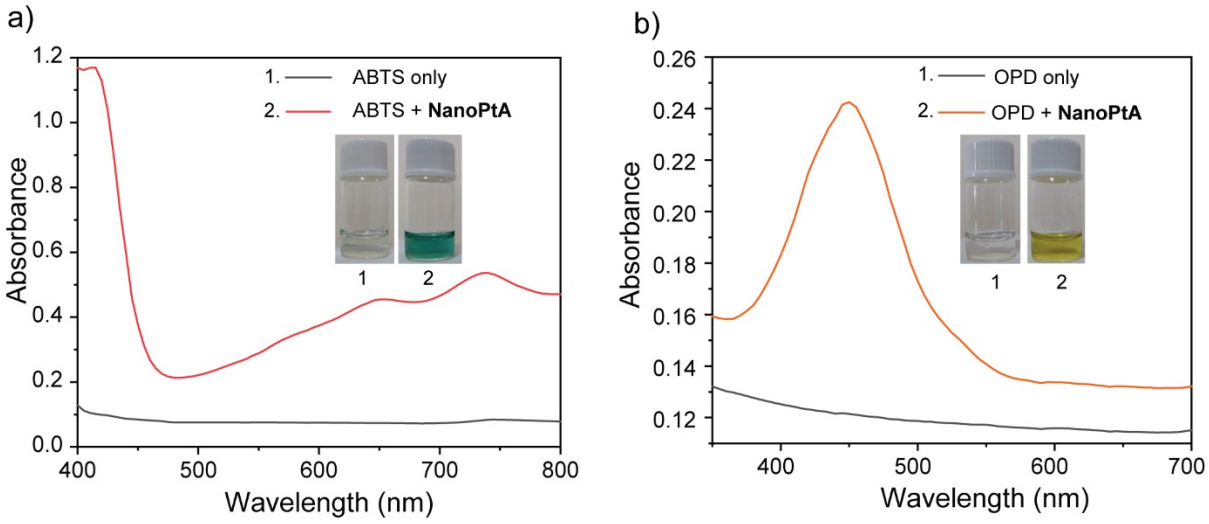

Fig. S21. (a,b) UV absorption spectra of ABTS (0.5 mM) and OPD (0.5 mM) in the presence of **NanoPtA** (10 µM) upon irradiation with visible light 470 nm for 10 min. in acetate buffer (100 mM, pH 4.0).

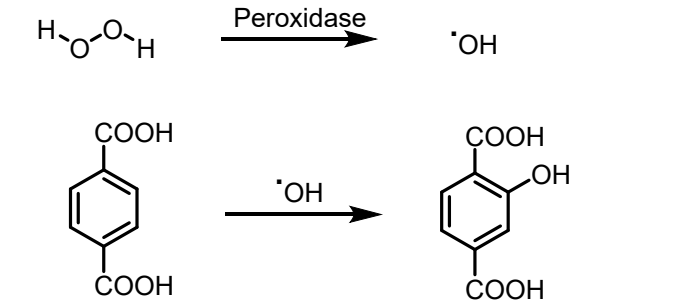

Terephthalic acid (TA)

2-Hydroxy terephthalic acid(TAOH) Emission at 435 nm

Scheme S3. Reactions involved in the terephthalic acid assay.

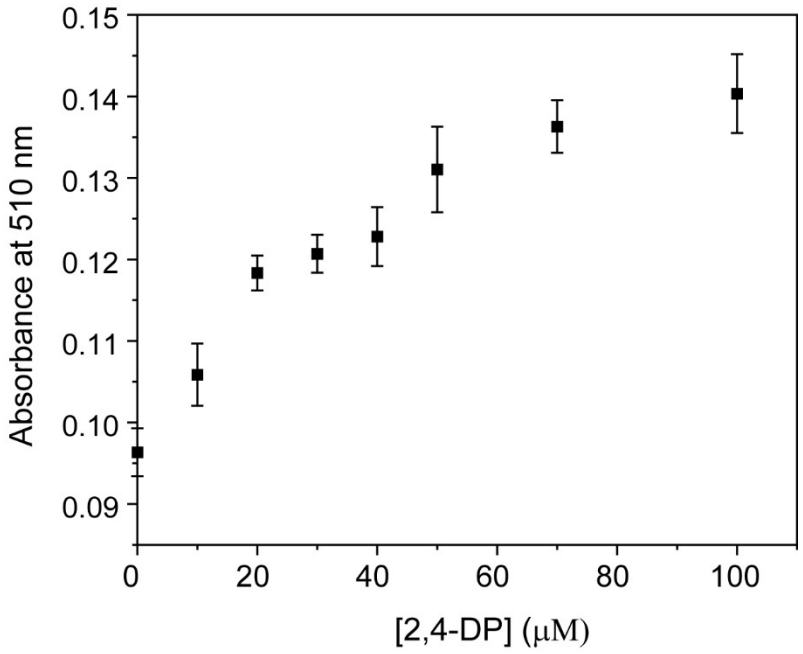

Fig. S22. Effect of 2,4 -DP concentrations on the catalytic activity of **NanoPtA** (10 μM) at 510 nm.

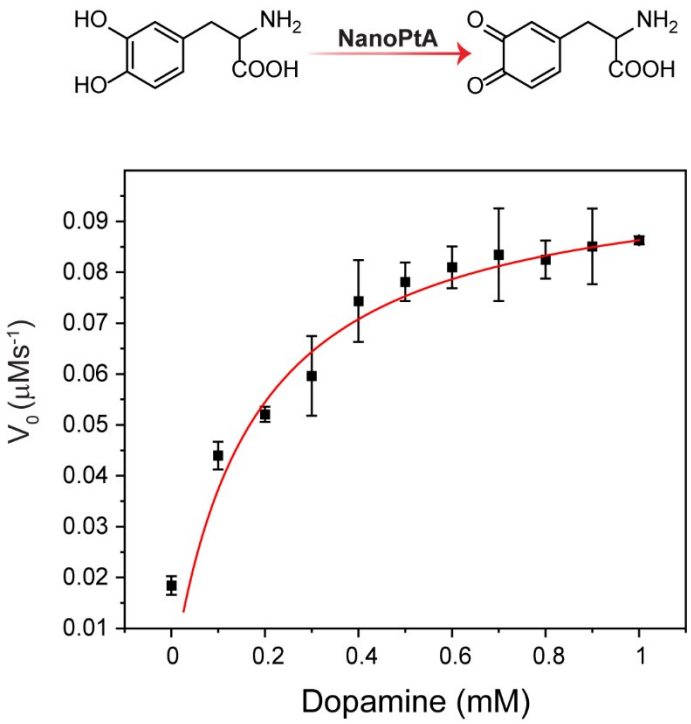

Fig. S23. Michaelis Menten plot of oxidized dopamine absorbance (at 475 nm) catalyzed by **NanoPtA** (10 μM) in HEPES buffer (10 mM, pH 7.4)**.** Light source = visible light 470 nm.

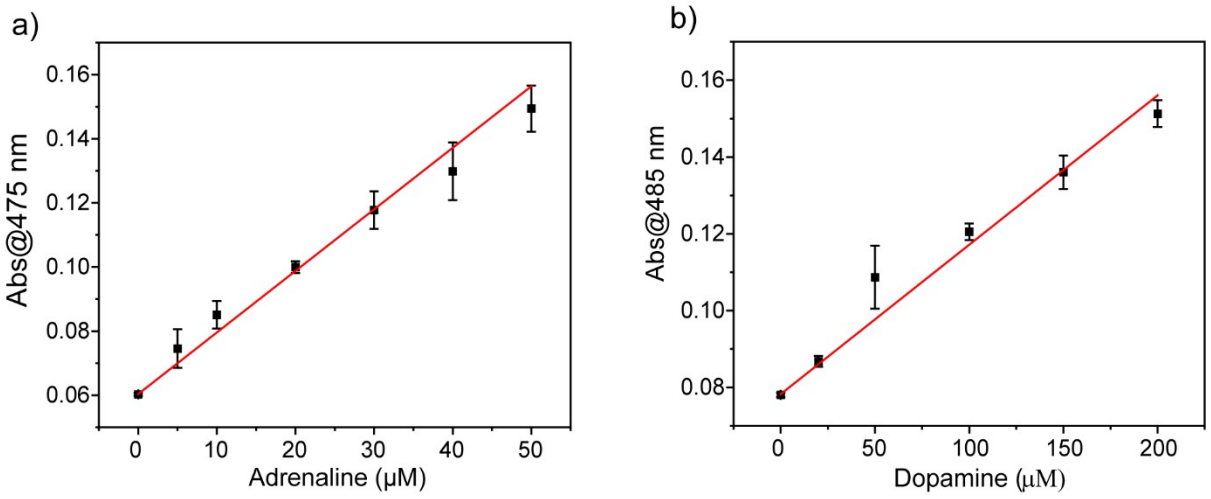

Fig. S24. (a) Plot of oxidized adrenaline absorbance at 475 nm versus adrenaline concentration catalyzed by **NanoPtA** (10 μM). (b) Plot of oxidized dopamine absorbance at 485 nm versus dopamine concentration catalyzed by **NanoPtA** (10 μM). The red line showed the linear fit of the data.

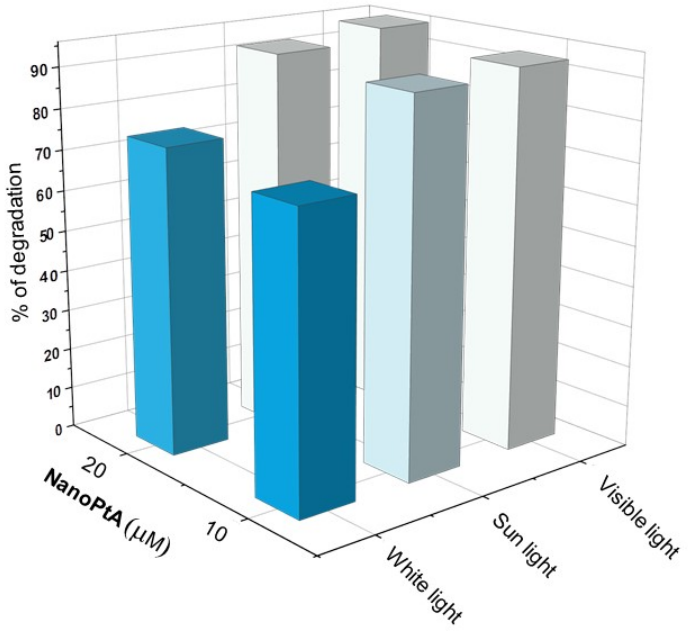

Fig. S25. Comparison of % trypan blue degradation under exposure to different irradiation sources in the presence of **NanoPtA** (10 μM and 20 μM). Light sources = Visible light at 470 nm, White light = 40W LED bulb, and Sunlight.

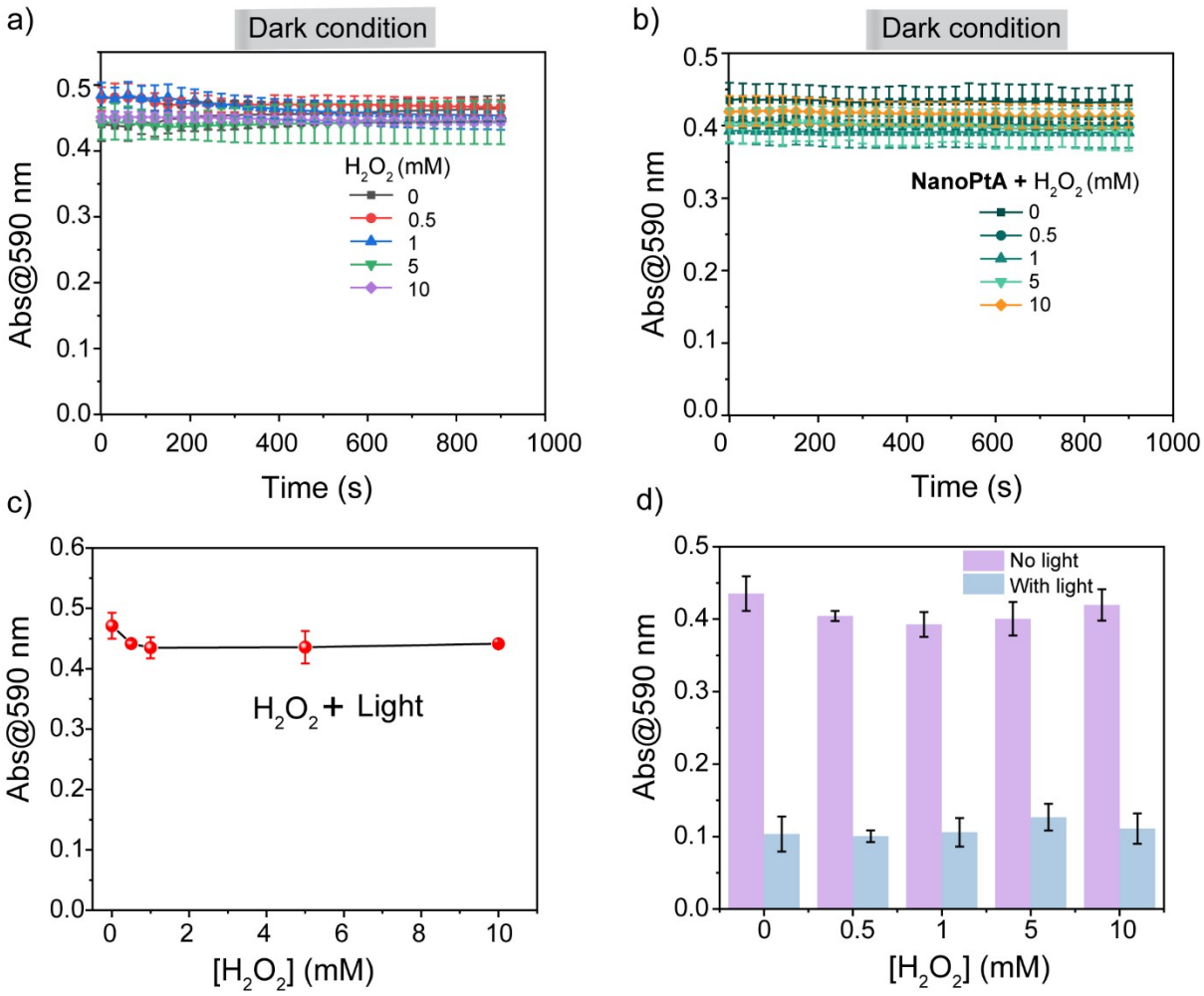

Fig. S26. (a) Absorbance at 590 nm for TrB dye degradation with time at various concentrations of H_2O_2 (0, 0.5, 1,5, 10 mM) in the absence of visible light. (b) absorbance at 590 nm for TrB dye degradation with time at various concentrations of H_2O_2 (0, 0.5, 1,5, 10 mM) with **NanoPtA** (10 μM) in the absence of visible light. (c) TrB dye degradation with time at various H_2O_2 concentrations (0, 0.5, 1,5, 10 mM) in the presence of visible light. (d) TrB dye degradation with **NanoPtA** (10 μM) at various H_2O_2 concentrations (0, 0.5, 1,5, 10 mM) in the absence and presence of visible light.

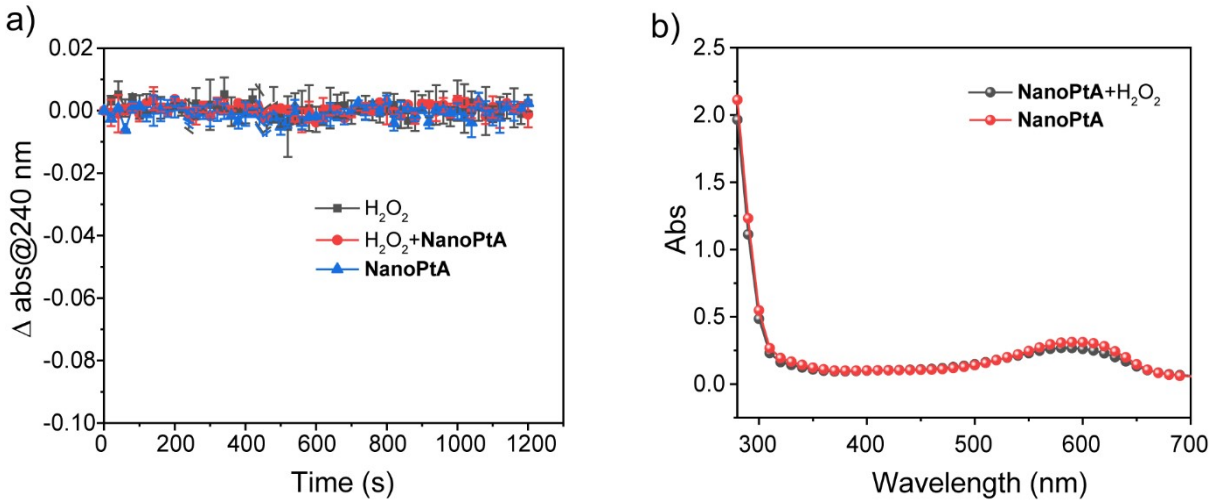

Fig. S27. a) Degradation of H_2O_2 (25 μM) in the presence of **NanoPtA** (10μM) over time b) Degradation of TrB dye (20 μM) in the presence of **NanoPtA** alone and H_2O_2 and **NanoPtA** mixture after degassing the vials with N_2.

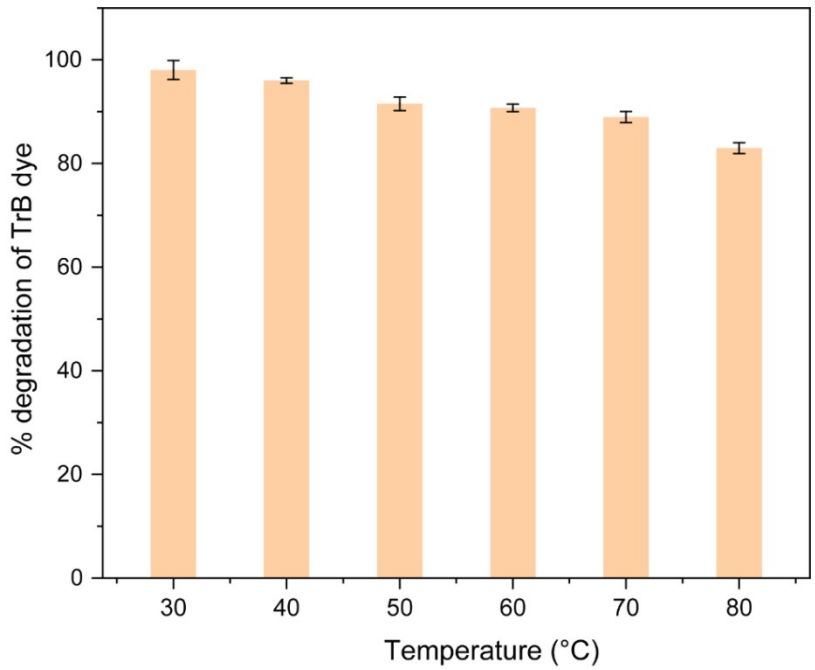

Fig. S28. Effect of temperature on % of trypan blue degradation.

Table S1. Comparison of the kinetic parameters between **NanoPtA** and reported oxidase, and oxidase-mimicking nanozymes.

Catalysts and Substrate	K_m (mM)	V_{max} (10^{-8} Ms^{-1})	Reference
Dex-FeMnzyme (TMB)	0.33	13.29	1
CeO_2 NPs (TMB)	3.8	70	2
Fe-N/C (TMB)	0.94	59.8	3
Fe-Co-LDH (TMB)	0.34	5.4	4
Fe single atom nanozyme (TMB)	0.13	2.25	5
Mn_3O_4 NPs (TMB)	0.025	5.07	6
Pd cage (TMB)	0.24	7.084	7
NanoPtA (TMB)	0.030	10.5	This Work

References

1. X. Han, L. Liu, H. Gong, L. Luo, Y. Han, J. Fan, C. Xu, T. Yue, J. Wang and W. Zhang, *Food Chem.*, 2022, **371**, 131115.
2. A. Asati, S. Santra, C. Kaittanis, S. Nath and J. M. Perez, *Angewandte Chemie International Edition*, 2009, **48**, 2308-2312.
3. Q. Chen, S. Li, Y. Liu, X. Zhang, Y. Tang, H. Chai and Y. Huang, *Sensors and Actuators B: Chemical*, 2020, **305**, 127511.
4. X. Xu, X. Zou, S. Wu, L. Wang, J. Pan, M. Xu, W. Shan, X. Li and X. Niu, *Microchimica Acta*, 2019, **186**, 815.
5. C. Zhao, C. Xiong, X. Liu, M. Qiao, Z. Li, T. Yuan, J. Wang, Y. Qu, X. Wang, F. Zhou, Q. Xu, S. Wang, M. Chen, W. Wang, Y. Li, T. Yao, Y. Wu and Y. Li, *Chemical Communications*, 2019, **55**, 2285-2288.
6. X. Zhang and Y. Huang, *Analytical Methods*, 2015, **7**, 8640-8646.
7. S. Bhattacharyya, S. R. Ali, M. Venkateswarulu, P. Howlader, E. Zangrando, M. De and P. S. Mukherjee, *Journal of the American Chemical Society*, 2020, **142**, 18981-18989.